Fabrication and characterisation of polymer thin-films derived from cineole using radio frequency plasma polymerisation

Christopher D. Easton [a], Mohan V. Jacob [a,*], Robert A. Shanks [b]

[a] Electronic Materials Research Lab, School of Engineering, James Cook University, Townsville 4811, Australia
[b] Applied Sciences, RMIT University, GPO Box 2476V, Melbourne 3001, Australia

ABSTRACT

The development of organic polymer thin-films is critical for the progress of many fields including organic electronics and biomedical coatings. This paper describes the fabrication of an organic polymer thin film produced from 1,8-cineole via radio frequency plasma polymerisation. A deposition rate of 55 nm/min was obtained under the polymerisation conditions employed. Infrared spectroscopic analysis demonstrated that some functional groups observed in the monomer were retained after the polymerisation process, while new functional groups were introduced. The refractive index and extinction coefficient were estimated to be 1.543 (at 500 nm) and 0.001 (at 500 nm) respectively. The polymers were shown to be optically transparent. AFM images of the polymer established a very smooth and uniform surface with average roughness of 0.39 nm. Water contact angle data demonstrated that the surface was stable while in contact with water.

© 2009 Elsevier Ltd. All rights reserved.

1. Introduction

The advent of thin-film applications stemming from new technologies including organic electronics [1] and bioelectronics [2] has resulted in an increase in attention in the development of polymer thin-films from organic resources. Plasma polymerisation is a method for fabricating organic thin-films for use in such applications using materials that do not normally polymerise using conventional techniques [3]. The resulting polymer is typically of a high quality, exhibiting properties including chemical and physical stability, film homogeneity and a smooth, pinhole free surface [4,5]. In addition, it is possible to maintain a high degree of chemical functionality of the monomeric precursor through control of the deposition parameters [6]. As a result, plasma polymerisation has become popular for use in the biomedical field for the fabrication of bio-reactive and non-bio-reactive coatings [7].

1,8-Cineole, or Eucalyptol, is a saturated monoterpene and it is major component of Eucalyptus oil. The chemical structure of 1,8-cineole is shown in Fig. 1. This monomer is obtained from a natural, environmentally friendly, non-petrochemical resource. Use of both Eucalyptus oil and 1,8-cineole as monomers within medical research has gained considerable interest in recent years. Examples include use as an anti-inflammatory in bronchial asthma [8],

inhibition of cytokine production [9], and induce activation of human monocyte derived macrophages, stimulating their phagocytic response and thus inducing an immune system response [10]. The antifungal activity of 1,8-cineole has been confirmed via biofilm experiments [11].

Plasma polymerisation has been implemented in the past to fabricate films from Eucalyptus oil [12], where the electrical and optical (optical band gap) properties of the films were examined. However, as Eucalyptus oil is a mixture of several components with different vapour pressures, it is not clear which components contributed to the formation of the polymer within the plasma phase. The plasma polymerisation process involved fragmentation of the monomer molecules upon release into the plasma phase, and thus not only 1,8-cineole, but the additional components found in Eucalyptus oil will contribute to the composition of the resulting polymer.

The aim is to fabricate polymer thin-films from 1,8-cineole via plasma polymerisation and determine the chemical, optical, surface and physical properties of the resulting films. The chemical structure of the polymer will be investigated using Fourier transform infrared (FTIR) spectroscopy. Spectroscopic ellipsometry will be employed to determine the refractive index, extinction coefficient and optical transmission of the material. Ellipsometry will also be utilised to monitor the thickness of the resulting films and evaluate the deposition rate of the polymer thin-film. Atomic force microscope (AFM) will be used to study the surface profile of the polymer films, and the physical properties of the surface will be examined via water contact angle (WCA) measurements.

* Corresponding author. Tel.: +61 7 47814379; fax: +61 7 47815177.
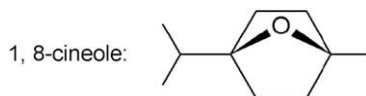E-mail address: mohan.jacob@jcu.edu.au (M.V. Jacob).

1, 8-cineole:

Fig. 1. Chemical structure of 1,8-cineole.

2. Experimental

1,8-Cineole monomer obtained from Australian Botanical Products was used for the fabrication of the plasma polymer thin-films at a radio frequency (RF) power level of 25 W and for various deposition times. The deposition parameters including RF power and pressure employed in this study were adapted from a previous study [13]. A diagram of the experimental apparatus is presented in Fig. 2. The polymer films were fabricated at a pressure of approximately 33 Pa. RF energy (13.56 MHz) was delivered to the deposition chamber via external copper electrodes separated by a distance of 11 cm. The distance between the monomer inlet and the edge of the plasma excitation zone (edge of right electrode in Fig. 2) was 12 cm. Approximately 1 mL of the monomer is placed into the holder and replaced after each subsequent deposition. The monomer inlet was opened in order to evacuate the monomer container prior to placement of substrate within the polymerisation cell. The monomer was released into the chamber throughout deposition, and the flow rate was controlled via a vacuum stopcock. It was found that for the cineole monomer addition, completely opening the monomer flow valve lead to saturation of the polymerisation cell and resulted in a pressure too high for polymerisation. Therefore greater control of the flow rate was required when using this monomer compared with the previous study in order to achieve the same deposition pressure. To achieve this, the monomer flow rate was restricted by only opening the valve partially. The monomer flow rate was determined employing the procedure outlined by Gengenbach and Griesser [2]. Briefly, the flow rate (F; cm^3 (STP)/min) was determined using the following equation [3]:

$$F = \frac{dp}{dt} \times 16172 \frac{V}{T} \qquad (1)$$

where p = pressure (mbar), t = time (s), V = volume of plasma reactor = 1.8 L, T = temperature = 295 K. The change in pressure as a function of time was determined by first evacuating the plasma reactor, then opening the monomer valve and allowing the pressure to stabilise. The valve to the vacuum pump was then closed and the pressure recorded every 5 s for 60 s. A flow rate of $F = 1.26$ cm^3/min was employed in this study.

Three different types of substrate were employed in this study; glass slides for AFM, Ellipsometry and WCA experiments, the films were deposited onto KBr directly for FTIR analysis, and NaCl disks were used for FTIR of the 1,8-cineole monomer. The glass slides were first cleaned with a solution of extran and distilled water, then ultrasonically cleaned for 15 min, rinsed with propan-2-ol and air-dried. The wet cleaning procedure was not employed for the KBr discs. Prior to fabrication, all substrates were pre-treated with Ar plasma in order to produce an oxygen-free surface [4].

FTIR spectroscopy was employed to determine the chemical structure of the polymer thin-films using a Perkin–Elmer Spectrum 2000 FTIR Spectrometer. Spectra were obtained in transmission mode in the region of 4000–500 cm^{-1}, where 32 scans were acquired for each sample at a resolution of 1 cm^{-1}. CO_2 and H_2O were eliminated from spectra by a background substraction procedure, where the background was pre-recorded under the same atmospheric conditions.

Optical properties and thickness of the resultant thin-film were examined over the wavelength range 190–1000 nm using a variable angle spectroscopic ellipsometer (model M-2000, J. A. Woollam Co., Inc.). Ellipsometric parameters Ψ and Δ were obtained at three different angles of incidence, $\varphi = 55°$, $60°$, and $65°$. In addition, the transmission data was also collected. Ψ and Δ were used to derive the optical constants based on a model of the sample built in the J.A. Woollam Inc. analysis software (WVASE32) via regression analysis. The quality of the fit was measured quantitatively by determining the mean-squared error and through the use of the correlation matrix. Gaussian and Tauc-Lorentz oscillators were employed within the model to provide an optimal fit of the data, with a lower mean square error and lower average correlation between fitting terms. A more detailed review of the procedure has been reported elsewhere [14].

Analysis of the surface morphology was undertaken using the NT-MDT NTEGRA Prima AFM in semi-contact mode.

Water contact angle measurements were performed using a KSV 101 system. The height of each drop is confirmed using a CCD camera prior to each measurement to ensure consistency in drop volume. Drop volumes of approximately 8 μL were employed, where 8 drops were used to determine the WCA. Double distilled water produced using a Labglass Delta system (Labglass Pty Ltd) was employed for the measurements. Once the drop was placed on the surface using a one-touch dispenser system, the KSV CAM software was triggered to begin recording. An image was recorded every second for 30 s in order to monitor the contact angle as a function of time. Image processing software was used to determine the contact angle by fitting the measured drop profile with the Young–Laplace equation.

3. Results and discussion

3.1. Deposition rate

Polymer thin-films were successfully fabricated from 1,8-cineole using an RF glow discharge. Spectroscopic ellipsometry was employed to determine the thickness of the polymer, and the estimated film thickness as a function of time is demonstrated in Fig. 3. This study demonstrated that a deposition rate of approximately 55 nm/min was achieved, which is comparable to deposition rates for other monomer precursors employed in plasma polymerisation such as thiophene [15]. The rate of deposition of polymer could be adjusted by altering the deposition parameters such as RF power or pressure, however the parameters outlined in experimental were maintained to allow for reproducibility. The deposition rate obtained indicates that thin film coatings can be fabricated in a minimal amount of time, leading to fast production rates for implementation in applications.

3.2. Infrared spectroscopic analysis

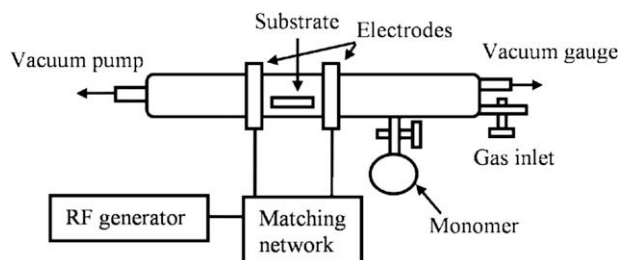FTIR spectra of 1,8-cinole monomer in addition to the 1,8-cineole based polymer films are presented in Fig. 4 with the
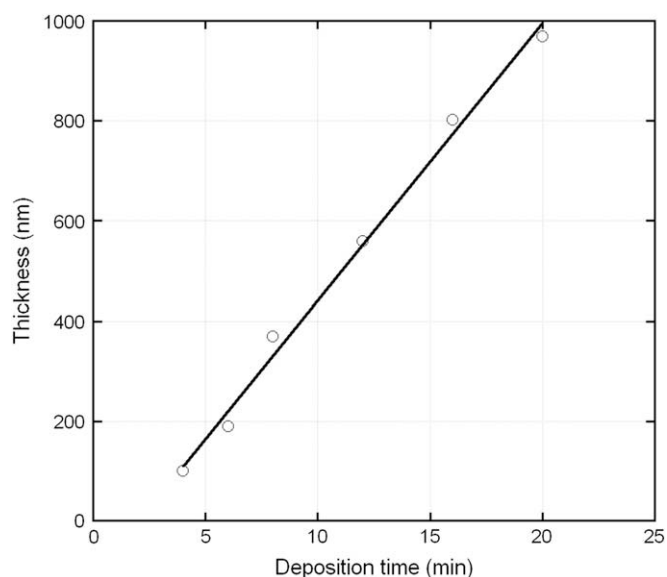
Fig. 2. Experimental apparatus.

Fig. 3. Thickness of 1,8-cineole based polymer thin-film as a function of deposition time.

Table 1
FTIR spectra assignments for 1,8-cineole monomer and 1,8-cineole based polymer. Vibrational modes: ν_a = asymmetrical stretching, ν_s = symmetrical stretching, ν = stretching, δ_a = asymmetrical bending, δ_s = symmetrical bending.

Wavenumber (cm^{-1})	Relative intensity	Assignment
1,8-Cineole monomer:		
~3175 (broad)	Very weak	ν(O–H)
~2985, ~2968, ~2945, ~2924	Very strong	ν_a(C–H)
~2881	Strong	ν_s(C–H)
~2853	Medium	ν_s(C–H)
1466 and 1446	Medium	δ(C–H)
1375	Strong	δ_s(C–H)
1359	Medium	δ(C–H)
1307	Medium	ν(C–C)
1272	Weak	ν(C–C)
1232	Medium	ν(C–C)
1214	Strong	ν(C–C)
1168	Medium	ν(C–O)
1081	Strong	δ(C–H)
1052	Medium	δ(C–H)
1015, 986, 929, 921, 888, 864, 843, 812, 788, 765, 650, 576	Very strong to very weak	C–H deformation
1,8-Cineole based polymer		
~3469	Weak	ν(O–H)
2958 and 2930	Very strong	ν_a(C–H)
2872	Medium	ν_s(C–H)
1707	Weak	ν(C=O)
1456	Weak	δ_a(C–H)
1375	Weak	δ_s(C–H)
1213	Very weak	ν(C–C)
1163	Very weak	ν(C–O)
1059	Very weak	δ(C–H)
986	Very weak	CH deformation

corresponding FTIR assignments listed in Table 1 based on the peak assignments presented in Ref. [16]. Considering first the spectrum for the monomer, the spectral allocation was expected to be straightforward as the chemical structure was known. Stretching of methyl (2985 cm^{-1}, 2968 cm^{-1}, 2945 cm^{-1}, and 2881 cm^{-1}) and methylene groups (2924 cm^{-1} and 2881 cm^{-1}) is indicated by strong bands in the spectrum, in addition to bending of C–H groups (1466 cm^{-1}, 1446 cm^{-1}, 1375 cm^{-1}, 1081 cm^{-1}, and 1052 cm^{-1}). Bands between 1359 cm^{-1} and 1214 cm^{-1} demonstrate stretching of carbon–carbon bonds. C–O stretching is represented by the peak at 1168 cm^{-1}, while the very weak peak at 3175 cm^{-1} assigned to O–H stretching could imply an impurity.

Comparison of the results for the 1,8-cineole based polymer with that of the monomer, it is apparent that upon polymerisation the intensity of the bands within the fingerprint region have been reduced, however some functional groups of the monomer were maintained. The bands around 2900 cm^{-1} associated with methyl and methylene groups appear largely unaffected. The broad peak at
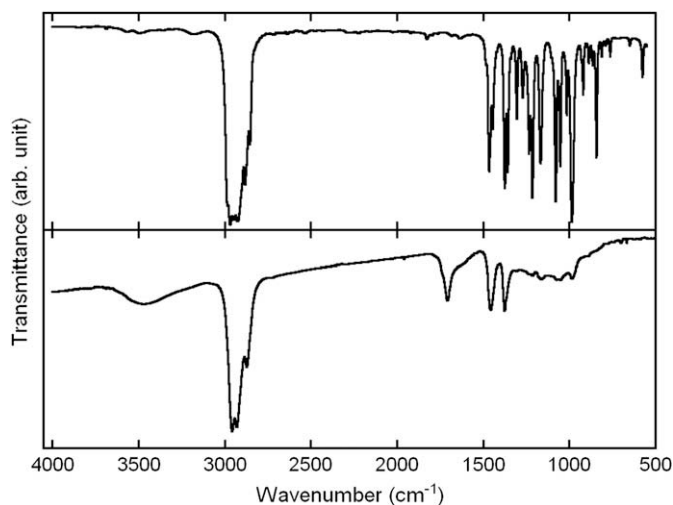

Fig. 4. FTIR spectra of 1,8-cineole monomer (top spectrum) and 1,8-cineole based polymer (bottom spectrum).

3469 cm^{-1} is associated with O–H stretching, while the peak at 1707 cm^{-1} is indicative of C=O of ketone, which was not present in the monomer spectra. An ether group is present in the monomer, and this can be converted to other oxygen containing species, such as a ketone group in the polymer. Within the plasma phase, fragmentation of parts of the monomer occurs. If one or both bonds of the between the oxygen and carbon in the ether group can be ruptured within the plasma, then this could lead to the oxygen forming a double bond with a single carbon group to become stable and thus form the ketone. As the ketone groups are present in the polymer, it would appear that this reaction path is favourable. Carbon–carbon bonds by analogy become unsaturated by plasma treatment. Therefore based on the assigned spectra, the resultant polymer was predominantly hydrocarbon dense with the presence of oxygen containing groups in the form of alcohol and ketone groups within the structure.

3.3. Optical properties

In addition to the thickness measurements, ellipsometry was utilised to determine the optical properties of the polymer. Refractive index and extinction coefficient of the polymer for various thicknesses were measured, in addition to the transmission of the polymer and glass slide, and they are shown in Fig. 5. The refractive index of the 1,8-cineole polymer was slightly greater than that of the glass slide, while the extinction coefficient demonstrated that there was negligible absorption at wavelengths greater than 400 nm. The polymer was shown to be optically transparent, as revealed by the transmission data. At low wavelength, a deviation occurs with respect to thickness for the measured optical parameters. Both the refractive index and extinction coefficient tended to increase with increasing thickness at approximately 200 nm, while the transmission tended to decrease with increasing thickness at approximately 350 nm. This deviation was however insignificant and
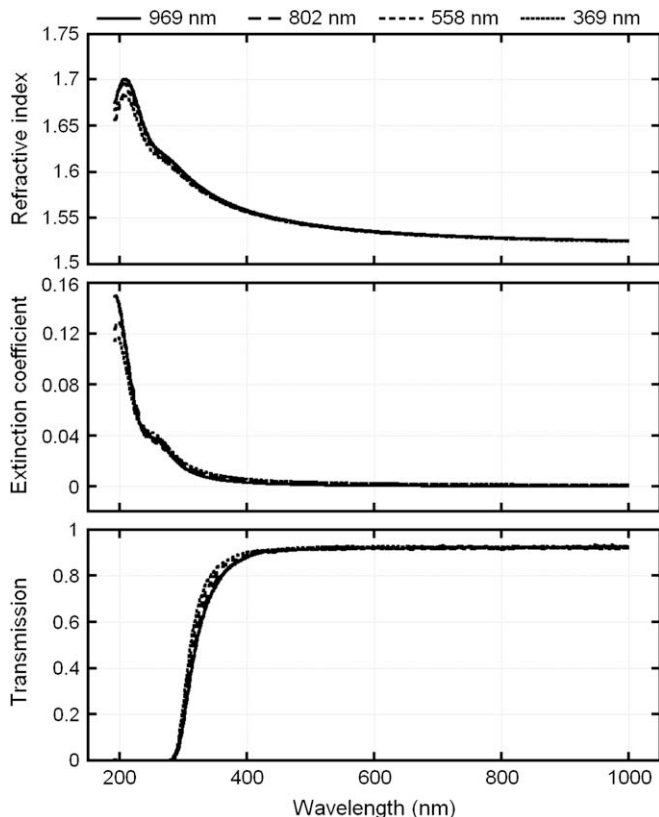
Fig. 5. Refractive index (top panel) and extinction coefficient (middle panel) of the 1,8-cineole based polymer film and transmission (bottom panel) of polymer and substrate.

restricted to a small wavelength region, and thus for the thickness range measured, the optical constants of the 1,8-cineole polymer film were independent of thickness. It will be possible to tailor the optical properties to suit different optical applications by changing the deposition parameters.

The optical band gap (E_O) was derived using absorption coefficient data obtained from spectroscopic ellipsometry measurements
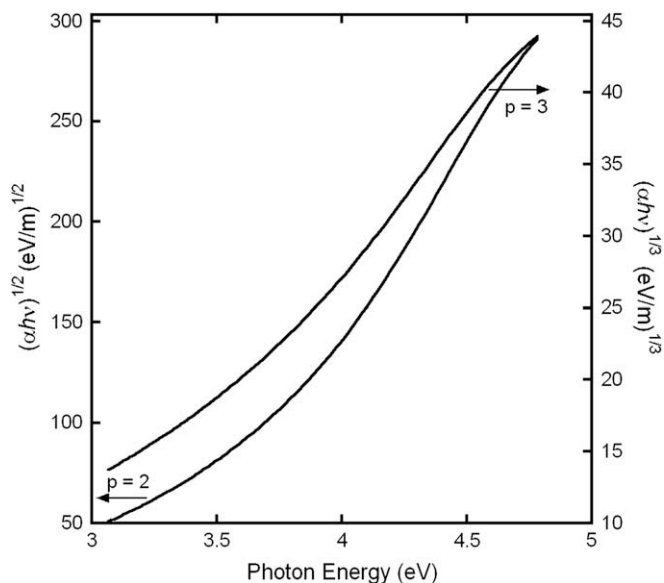
using the procedure outlined previously [14]. Briefly, E_O is calculated using the Tauc relation [17]:

$$\alpha h\nu = B(h\nu - E_O)^p \qquad (2)$$

where $h\nu$ is the energy of light, p is a constant connected to the density of states, and B is linked to the length of localised state tails. p can have values of 2, 3, ½, etc. depending on the nature of the electronic structure. Fig. 6 demonstrates the fit for $p = 2$ and $p = 3$ for the cineole based polymer sample. It was found that $p = 3$ provided the best fit, resulting in $E_O = 2.83$ eV.

3.4. AFM study

AFM images were obtained in semi-contact mode of the 1,8-cineole based polymer films to provide information on the surface of the polymer. An image of the film with scan size 1×1 μm is presented in Fig. 7. Scan size of 10×10 μm is not shown, however, was employed for determining the average roughness for the film surface. An average roughness of 0.39 nm was obtained for the films using AFM, and this compared favourably with that obtained from ellipsometry (0.37 nm). Both the image and the roughness results indicate that the surface was very smooth and uniform.

3.5. Water contact angle

The equilibrium contact angle was determined using a KSV 101 system. As outlined previously [18], the experimental procedure was confirmed by measuring the WCA of polytetrafluoroethylene, where the data was represented by a linear fit with equation $y = -0.01t + 119.95$ and $R^2 = 0.97$, where t represents time. Fig. 8 demonstrates the water contact data for the 1,8-cineole polymer film, where the error bars in the plot represent 95% confidence levels at each time interval. Extrapolating the line of best fit to time zero resulted in a WCA of 89.8°. The generally accepted cutoff between a hydrophilic and hydrophobic surface is 90°, though this is an arbitrary value The range of WCA values obtained are on the proposed borderline between hydrophobic and hydrophilic, therefore based on this criteria alone it was difficult to assign the polymer as either hydrophilic or hydrophobic. However, at the contact angle values recorded, beading of the water droplets was observed, suggesting the surface was more likely mildly hydrophobic.

Within the first few seconds after initial contact with the surface, the rate of change in contact angle differed from the remainder of the measurements. An initial rapid rate of change in contact angle was typically assigned to absorption of water by the sample [19]. However the deviation of the data from the line of best
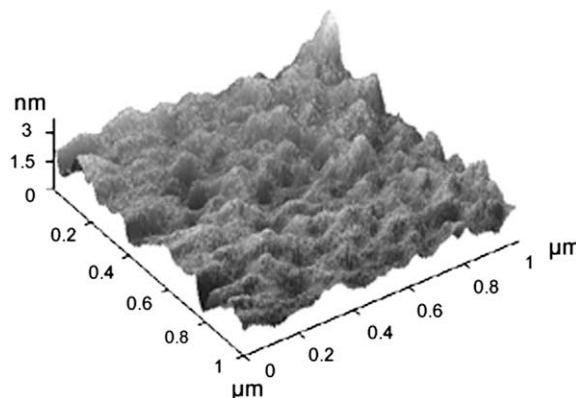

Fig. 6. Absorption edge of 1,8-cineole based polymer obtained from ellipsometric data, derived from Equation (2) for $p = 2$ and $p = 3$.

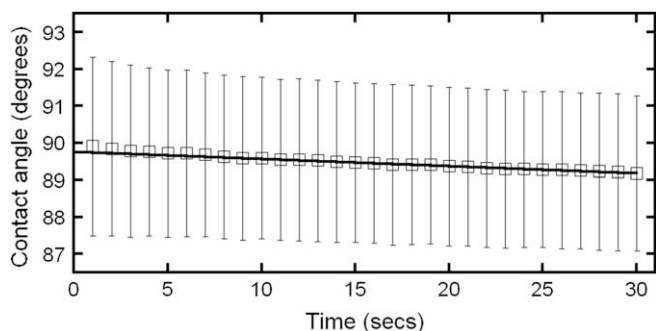**Fig. 7.** AFM image (1×1 μm) of 1,8-cineole based polymer film.

Fig. 8. Water contact angle versus time for the 1,8-cineole based polymer.

fit at the beginning of the experiment was minimal as shown in the case of the 1,8-cineole polymer. In addition, the line of best fit was given by the equation $y = -0.0197t + 89.771$, which indicated that the change in water contact angle in this study was $-0.02° \, s^{-1}$, compared with $-0.2° \, s^{-1}$ for poly(acrylic acid) [19]. These results indicated that it was highly unlikely that interactions such as swelling or reorientation of polar groups were occurring at the liquid–solid interface, and thus the 1,8-cineole polymer was structurally stable while in contact with water. It has been demonstrated previously [20] that plasma polymerised films with contact angles between 60 and 90° provide favourable dose response of ^{125}I-protein A uptake to human immunoglobulin G (hIgG). Based on the results presented here, the 1,8-cineole polymer has the potential to be employed in biomedical applications. If the antimicrobial activity of the 1,8-cineole monomer could be maintained during the polymerisation process then the resulting polymer could be employed as a non-bio-reactive coating. This would allow fabrication of surface coatings for medical devices without the need for additional processing to include an antimicrobial component, such as a silver ion filler [21].

4. Conclusion

Polymer thin-films have been fabricated from the saturated monoterpene 1,8-cineole and the properties of the material have been examined. The deposition rate was found to be approximately 55 nm/min, comparable with other precursors employed in plasma polymerisation. FTIR spectra of both the monomer and resultant polymer have been examined. Some of the functional groups observed in the monomer were retained during the polymerisation process by comparison the two spectra. C–H stretching and bending associated with methyl and methylene groups were present in the polymer, in addition to C=O stretch assigned to ketone and O–H stretch indicating the presence of alcohol. The optical properties of the polymer were investigated using ellipsometry. Transmission spectra of the films confirmed that they were optically transparent. The refractive index of the polymer was only slightly greater than

that of glass, while the extinction coefficient demonstrated that there was no absorption at wavelengths greater than 400 nm. All optical parameters measured were found to be independent of thickness within the range measured. An optical band gap of $E_O = 2.83 \, eV$ was measured. AFM investigation of the polymer demonstrated a surface that was very smooth and uniform, with an average roughness of 0.39 nm, confirmed by ellipsometry. Water contact angles for the polymer demonstrated that the surface was structurally stable. These results predict that the polymer could be employed in a number of applications including optoelectronic and biomedical. Use in applications such as a non-bio-reactive coating however requires additional study into the schemes to maintain and enhance the antimicrobial nature of the monomer during polymerisation.

References

[1] Vardeny ZV, Heeger AJ, Dodabalapur A. Synthetic Metals 2005;148(1):1–3.
[2] Berggren M, Richter-Dahlfors A. Advanced Materials 2007;19(20):3201–13.
[3] Hiratsuka A, Karube I. Electroanalysis 2000;12(9):695–702.
[4] Kim MC, Cho SH, Han JG, Hong BY, Kim YJ, Yang SH, et al. Surface & Coatings Technology 2003;169:595–9.
[5] Sajeev US, Mathai CJ, Saravanan S, Ashokan RR, Venkatachalam S, Anantharaman MR. Bulletin of Materials Science 2006;29(2):159–63.
[6] Beck AJ, Jones FR, Short RD. Polymer 1996;37(24):5537–9.
[7] Forch R, Chifen AN, Bousquet A, Khor HL, Jungblut M, Chu LQ, et al. Chemical Vapor Deposition 2007;13(6–7):280–94.
[8] Juergens UR, Dethlefsen U, Steinkamp G, Gillissen A, Repges R, Vetter H. Respiratory Medicine 2003;97(3):250–6.
[9] Juergens UR, Engelen T, Racke K, Stober M, Gillissen A, Vetter H. Pulmonary Pharmacology & Therapeutics 2004;17(5):281–7.
[10] Serafino A, Vallebona PS, Andreola F, Zonfrillo M, Mercuri L, Federici M, et al. Bmc Immunology 2008:9.
[11] Dalleau S, Cateau E, Berges T, Berjeaud JM, Imbert C. International Journal of Antimicrobial Agents 2008;31(6):572–6.
[12] Kumar DS, Nakamura K, Nishiyama S, Noguchi H, Ishii S, Kashiwagi K, et al. Journal of Applied Polymer Science 2003;90(4):1102–7.
[13] Jacob MV, Easton CD, Woods GS, Berndt CC. Thin Solid Films 2008;516(12):3884–7.
[14] Easton CD, Jacob MV. Thin Solid Films 2009;517(15):4402–7.
[15] Silverstein MS, Visoly-Fisher I. Polymer 2002;43(1):11–20.
[16] Coates J. In: Meyers RA, editor. Interpretation of infrared spectra, a practical approach. Chichester, UK: John Wiley & Sons Ltd; 2000. p. 10815–37.
[17] Tauc J, Grigorovici R, Vancu A. Physica Status Solidi (b) 1966;15(2):627–37.
[18] C.D. Easton, M.V. Jacob, R.A. Shanks, B.F. Bowden. Chemical Vapor Deposition, in press. doi:10.1002/cvde.200806719.
[19] Alexander MR, Duc TM. Polymer 1999;40(20):5479–88.
[20] Kurosawa S, Kamo N, Minoura N, Muratsugu M. Materials Science and Engineering: C 1997;4(4):291–6.
[21] Kumar R, Howdle S, Munstedt H. Journal of Biomedical Materials Research Part B-Applied Biomaterials 2005;75B(2):311–9.